Electronic Structure of Heavy Halogen Atoms Adsorbed on the Cu(111) Surface: A Combined ARPES and First Principles Calculations Study

Won June Kim, Sarah Xing, Geoffroy Kremer, Muriel Sicot, Bertrand Kierren, Daniel Malterre, Giorgio Contini, Julien Rault, Patrick Le Fèvre, François Bertran, et al.

C: Surfaces, Interfaces, Porous Materials, and Catalysis

Electronic Structure of Heavy Halogen Atoms Adsorbed on the Cu(111) Surface: A Combined ARPES and First Principles Calculations Study

Won June Kim, Sarah Xing, Geoffroy Kremer, Muriel Sicot, Bertrand Kierren, Daniel Malterre, Giorgio Contini, Julien Rault, Patrick Le Fevre, Francois Bertran, Dario Rocca, Yannick Fagot-Revurat, and Sébastien Lebègue

J. Phys. Chem. C, **Just Accepted Manuscript** • DOI: 10.1021/acs.jpcc.9b07057 • Publication Date (Web): 09 Oct 2019

Electronic Structure of Heavy Halogen Atoms Adsorbed on the Cu(111) Surface: a Combined ARPES and First Principles Calculations Study

Won June Kim,[*,†] Sarah Xing,[‡,¶] Geoffroy Kremer,[‡] Muriel Sicot,[‡] Bertrand Kierren,[‡] Daniel Malterre,[‡] Giorgio Contini,[§,‖] Julien Rault,[⊥] Patrick Le Fèvre,[⊥] François Bertran,[⊥] Dario Rocca,[†] Yannick Fagot-Revurat,[*,‡] and Sébastien Lebègue[*,†]

†*Laboratoire de Physique et Chimie Théoriques LPCT (UMR CNRS 7019), Faculté des Sciences et Techniques, Université de Lorraine, BP 70239, Boulevard des Aiguillettes, 54506 Vandoeuvre-lès-Nancy CEDEX, France*

‡*Institut Jean Lamour, UMR 7198, CNRS-Université de Lorraine, CAMPUS ARTEM, 2 Allée André Guinier, BP 50840, 54011 Nancy, France*

¶ *CRYOSCAN, 2 Allée André Guinier, Campus ARTEM, 54011 Nancy, France*

§*Instituto di Struttura della Materia, CNR, Via Fosso del Cavaliere 100, 00133 Roma, Italy*

‖ *Department of Physics, Unversity of Rome Tor Vergata, Via della Ricerca Scientifica 1, 00133 Roma, Italy*

⊥*Synchrotron SOLEIL, Saint-Aubin, BP 48, F-91192 Gif-sur-Yvette Cedex, France*

E-mail: won-jun.kim@univ-lorraine.fr; yannick.fagot@univ-lorraine.fr; sebastien.lebegue@univ-lorraine.fr

Abstract

By means of angle-resolved photoemission spectroscopy (ARPES) and density functional theory (DFT) calculations, we investigate the electronic structure of a Br or I atom overlayer on the Cu(111) surface produced by the well known Ullmann coupling reaction. We found that the iodine adsorbate induces two spin-orbit splitted highly dispersive bands, which are well-separated from the bulk Cu-3d bands, whereas the bromine-induced bands are flat and largely hybridized with the copper states. Also, our measured constant energy maps show that the I-induced bands have a parabolic shape in the whole surface Brillouin zone, which is confirmed by our calculations. Overall, the agreement between theory and experiments is excellent, giving new insights concerning the electronic structure of halogen atoms on noble metals and its possible influence on the molecular electronic structure.

Introduction

The adsorption of halogen atoms on noble metal surfaces has been the subject of an intense research work in the field of surface science and electrochemistry in the last two decades. This is due to the fact that the adsorption of halogen atoms modifies the electronic structure and changes the surface work function, which is directly related to the electrochemical potential of the metal electrode.[1,2] Therefore, there have been several theoretical[3–16] and experimental[17–23] studies to investigate the overlayer structures, to measure the changes in the work function, and to study their dependence on the coverage of the halogen adsorbates. Especially, some recent works have focused on the relationship between the direction of the work function shift and the character of the metal-halogen bonding,[11,13] as well as the physical reasons for the formation of the particular patterns at low coverages.[20–23]

Also, halogen atoms, especially bromine and iodine, are the key ingredients of the well-known Ullmann coupling reaction, which is one of the chemical reaction that synthesizes organic or organometallic polymers on a metal surface.[24–26] In the Ullmann coupling reaction,

the deposition of halogenated molecules on noble metals leads to the formation of polymeric architectures, i.e., a molecular layer in a one or two-step reaction involving organometallic intermediates depending on the molecule/substrate affinity.[27–32] Changing the type of halogen in the precursor is known to lead to strong modification of the Ullmann reaction parameters, mainly due to its reactivity with the surface and its ability to participate to the final molecular architecture.[33] Indeed, depending on the size of the precursive halogenated molecules, halogen atoms remaining at the surface as a by-product of the reaction play a role both in the nanopatterning of the polymeric layer and possibly on the corresponding electronic structure.[34]

Therefore, understanding the electronic structure of halogen-adsorbed metal surface is fundamentally important for deep studies of the above phenomena. Regardless of this importance, the direct measurement of the band structure of halogen atoms on the metal surfaces have not been conducted up to now. In this letter, we focus on the modification of the electronic structure of the Cu(111) surface when two halogen atoms, I and Br, are adsorbed, by using combined experimental and theoretical methods. Firstly, we have synthesized molecular layer structures from the deposition of 1,4-diiodobenzene (dIB) and 1,4-dibromobenzene (dBB) on the Cu(111) surface and we confirmed the existence of patches of I/Br overlayer structures in them. Then the electronic structure of the I/Br-adsorbed Cu(111) overlayers are analyzed by both angle-resolved photoemission spectroscopy (ARPES) measurements and density functional theory (DFT) simulations.

Methods

Experimental Setup

All the experiments have been performed under ultra-high vacuum (UHV) conditions (base pressures below 2×10^{-10} mbar). The Cu(111) surface was prepared before dosing by multiple cycles of Ar^+ sputtering at 700 eV followed by annealing at 500 °C. The dIB and dBB

precursor molecules (Sigma-Aldrich, 98 % purity) were deposited from their crystallized forms in a quartz crucible by sublimation at room temperature onto the Cu(111) substrate (SPL Laboratory) through a leak valve. A partial pressure of 10^{-8} mbar was maintained in the chamber during few minutes while the substrate was kept at room temperature. The surface coverage was evaluated by recording STM images as function of sublimation time in our experimental set-up and by monitoring the XPS C-1s/Cu-2p peak intensity ratio on the CASSIOPEE beamline. Scanning tunneling microscope (STM) was performed with an Omicron LT-STM operating at liquid nitrogen or liquid helium temperatures, using a constant tunneling current, I, and a constant bias voltage, V_{BIAS}, measured from the tip to the sample (the tip is grounded). STM images were analyzed using WSxM software and treated for line-by-line flattening, plane subtraction and contrast enhancement. ARPES measurements were performed at the CASSIOPEE beamline of the synchrotron SOLEIL at a photon energy of 35 eV with an energy and momentum resolution of 10 meV and 0.01 Å^{-1} respectively, using a VG-SCIENTA R4000 analyzer. Light polarization in a linear horizontal configuration, i.e., electric field perpendicular to the sample surface, was taken. All the photoemission data were recorded at 30 K. LEED patterns were recorded at an electron energy of 145 eV and at a temperature of 80 K.

Computational Details

Our density functional theory (DFT) calculations were performed with the projector augmented wave (PAW) method as implemented in the Vienna *ab initio* Simulation Package (VASP).[35,36] The generalized-gradient approximation (GGA), as designed by Perdew, Burke, and Ernzerhof (PBE),[37] was used for the exchange-correlation functional and an energy cut-off of 600 eV was chosen for the plane wave basis set. Electronic iterations were continued until the total energy difference between steps became smaller than 10^{-7} eV, and the geometry optimization was performed until the force of each atom became smaller than 5.0×10^{-3} eV/Å.

To build a model for our calculations based on these previous experimental studies[17–19] and our STM/LEED measurements, we started by obtaining the equilibrium lattice parameter of bulk *fcc*-Cu. Our calculated lattice parameter $a = 3.63$ Å, obtained with a $12 \times 12 \times 12$ Γ-centered $\boldsymbol{k}$-point grid, is close to the experimental value of 3.615 Å.[38] The slab to model the Cu surfaces were constructed using the optimized lattice parameter of bulk Cu: we constructed a $\left(\sqrt{3} \times \sqrt{3}\right)R30^\circ$ supercell for the Cu(111) surface, with a thickness of eight atomic planes and we added a vacuum of 15 Å to avoid significant interactions between periodically repeated slabs. To have a similar grid spacing in the reciprocal space to that of the bulk calculation, we used a Γ-centered $\boldsymbol{k}$-grid of $10 \times 10 \times 1$. The geometry optimization of the surfaces (with and without adsorbates) were performed by constraining the four atomic layers at the bottom of the slab to reproduce the bulk geometry of Cu while the other atoms were allowed to relax freely. The adsorption energies of the Br and I adsorbate atoms on the different Cu surfaces were calculated by subtracting the sum of total energies of the clean surface and the isolated atom from the total energy of (atom+surface) structure. Relativistic effects have been taken into account in our band structure calculations, since spin-orbit coupling is expected to be significant. The constant energy maps were calculated by using a dense $\boldsymbol{k}$-point mesh of $30 \times 30 \times 1$.

Results and Discussion

Figures 1(a) and 1(c) show the STM images of the Cu(111) surface on which dIB and dBB precursors were used for the Ullmann coupling reaction, respectively. Even if I/Br patches and poly(*p*-phenylene) (PPP) or organometallic (OM) chains co-exist, the two precursors lead to different behaviors on the surface superstructure after the dehalogenation. When the dIB molecules are in contact with the Cu(111) surface and after a moderate annealing at 150 °C for 10 mn (see figure 1(a)), large areas of iodine domains (zone 1) including few PPP chains (zone 2) as well as ordered OM chains (zone 3) are evidenced by our STM

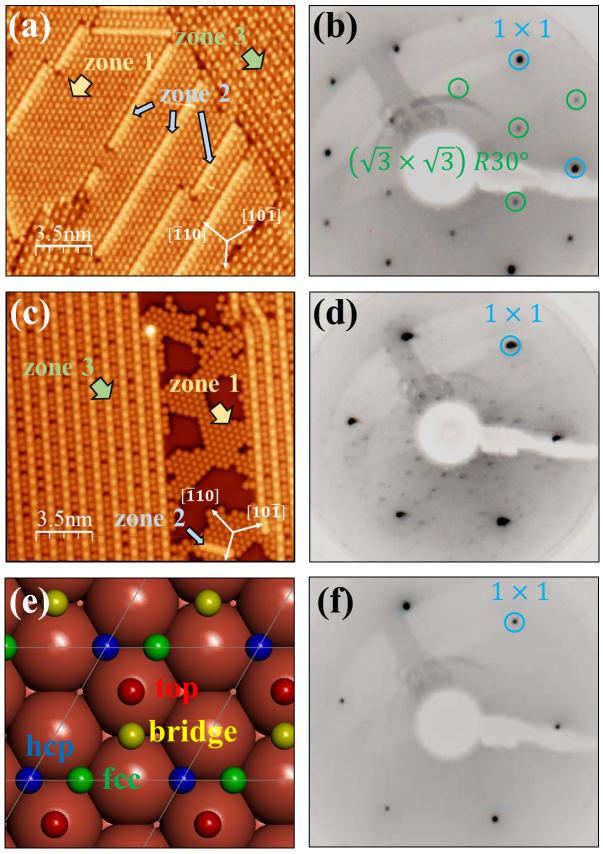

Figure 1: (a) STM image taken at 82 K on dIB/Cu(111) ($I = 0.34$ nA, $V_{\mathrm{BIAS}} = -0.39$ V) after deposition at room temperature and annealing for 10 mn at 150 °C; (b) corresponding $(\sqrt{3} \times \sqrt{3})R30°$ LEED pattern; (c) STM image taken at 5 K on dBB/Cu(111) ($I = 0.4$ nA, $V_{\mathrm{BIAS}} = -1.5$ V) after deposition at room temperature and annealing for 10 mn at 180 °C; (d) corresponding LEED pattern exhibiting the complex signature of the organometallic molecular reconstruction; (e) simulated $(\sqrt{3} \times \sqrt{3})R30°$ overlayer structure on the Cu(111) surface and possible adsorption sites of halogen atoms; (f) LEED pattern of the bare Cu(111) substrate used in this experiment. In the STM images, the areas of halogen patches, PPP chains, and OM chains are labeled as zone 1, 2, and 3, respectively.

mesurements. The PPP and OM chain periodicities of 4.4 and 6.8 Å are in agreement with previous works.[28,34] The iodine layer in zone 1 shows a periodicity of 4.4 Å, corresponding to that of $(\sqrt{3} \times \sqrt{3})R30°$ overlayer structure as expected from the periodicity of Cu(111) surface.

The low-energy electron diffraction (LEED) pattern of the dIB-deposited Cu(111) surface presented in figure 1(b) exhibits a well-defined $(\sqrt{3} \times \sqrt{3})R30°$ surface superstructure compared to that of the bare Cu(111) surface in figure 1(f). We interpret it as the signature of

the overlayer structure formed by iodine patches. On the other hand, the STM image of the dBB-deposited Cu(111) surface (see figure 1(c)) shows that Br domains are small compared to the iodine domains in the dIB-deposited Cu(111) surface. As a result, the domains of self-assembled OM chains also contribute to the LEED pattern leading to a more complex one as presented in figure 1(d). A more detailed analysis of this molecular self-assembling is beyond the scope of this paper and will be presented elsewhere for clarity. For the rest of the discussion, we use I/Cu(111) and Br/Cu(111) to either refer to the actual annealed surface of Cu(111) after adsorption of dIB and dBB, respectively or to the theoretical model of the corresponding halogen atoms on the Cu surface.

Table 1: Adsorption energies (in eV) and halogen-surface distances (in Å) of the I/Cu(111) and Br/Cu(111) overlayer structures. The most stable site for each composition is presented in bold.

Site	$\Delta E^{\mathrm{I}}_{\mathrm{ads}}$ (eV)	$r_{\mathrm{I-surf}}$ (Å)	$\Delta E^{\mathrm{Br}}_{\mathrm{ads}}$ (eV)	$r_{\mathrm{Br-surf}}$ (Å)
Top	-2.38	2.39	-2.65	2.27
3-fold *hcp*	-2.69	2.22	-3.01	2.03
3-fold *fcc*	**-2.70**	**2.22**	**-3.02**	**2.03**

Previous DFT studies have shown that for low coverages, both I and Br atoms occupy the 3-fold *fcc* site on the Cu(111) surface.[6,13,15] In our case, the measured LEED patterns of the $\left(\sqrt{3}\times\sqrt{3}\right)R30^\circ$ overlayer correspond to a coverage of 0.33 monolayer (ML) with a superperiodicity of 4.4 Å. To investigate the most stable sites and their consequences on the electronic structure, we calculated the adsorption energies (see table 1) of I and Br atoms for different sites using DFT. We have considered four different sites: top, 2-fold bridge, 3-fold *fcc* and *hcp* sites, as detailed in figure 1(e). Among them, 3-fold *fcc* is the most favorable site for both I and Br atoms, which is the same tendency as in previous DFT studies with lower coverages.[6,13,15] The 3-fold *hcp* site is less stable than 3-fold *fcc*, but the difference in the adsorption energies between the two sites is only 0.01 eV. Note that there is no value for the adsorption energy of the bridge site in table 1 since the I/Br atoms moved to the 3-fold *fcc* site during the geometry relaxation, indicating that this site is highly unfavorable.

From the ARPES measurements carried out on the I/Cu(111) surface shown in fig-

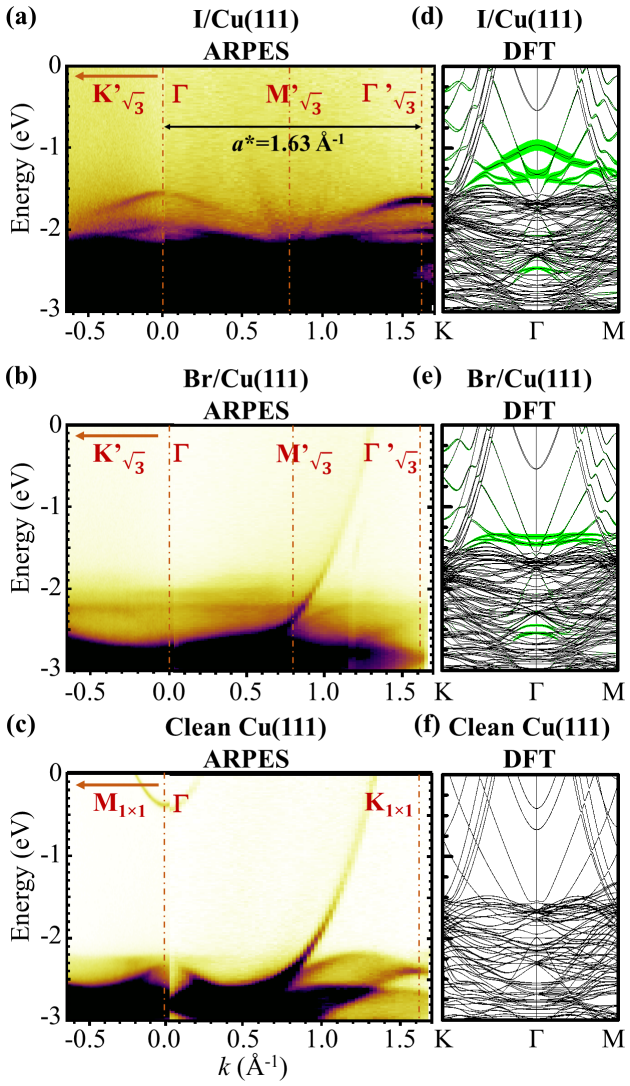

Figure 2: Left panels: ARPES intensity map measured at 30 K around the Γ point on (a) I/Cu(111), (b) Br/Cu(111), and (c) the bare Cu(111) substrate; Right panels: DFT band structures for (d) the I/Cu(111), (e) Br/Cu(111), and (f) clean Cu(111) surfaces. The green fatbands in figure 2(d) and 2(e) depicts the projection of the band structure onto the halogen atomic states. Fermi levels are set to zero for all figures.

ure 2(a), we found that two bands, separated by 0.48 eV, are clearly seen in the binding energy range between −1.6 to −2.2 eV below the Fermi level in comparison with the ARPES spectra obtained on the clean Cu(111) surface (figure 2(c)). These two bands have a parabolic shape centered at the Γ-point, and are well separated from the intense bulk Cu-3d bands. In addition, the maxima of these two bands are separated by 1.63 Å^{-1} along Γ-M-Γ as expected for the $(\sqrt{3} \times \sqrt{3})R30^\circ$ superperiodicity. On the contrary, the states which may be induced

by Br adsorbates are not clearly seen in the ARPES measurements considering the same energy range (see figure 2(b)). Notice that the two states that appear around -2 and -2.2 eV (see figure S2(a)) could originate either from the OM chains or from the Br layer.

To complement our analysis, we calculated the DFT band structures of the most stable configurations of the I/Cu(111) and Br/Cu(111) overlayers and compared with that of the clean Cu(111) surface, as presented in figures 2(d), 2(e), and 2(f), respectively, with the fatband projection of the halogen adsorbate states. Also, we present the same bandstructures but with highlighting the projection of the states of surface- and bulk-region Cu atoms in figure S1.

We found that the adsorption of a I or Br atom induces two major changes in the bandstructure. Firstly, I- or Br-derived bands are induced just above the Cu-3d bands when the atoms are adsorbed on the surface, as shown in figures 2(d) and 2(e). These induced bands are contributed mainly by the atomic states of the I or Br adsorbates, which are hybridized with the 3d atomic states of the surface Cu atoms (compare figures 2(d)-(e) with figures S1(b)-(c)). Interestingly, the I-induced and Br-induced bands have a different behavior, even though the Br and I atoms occupy the same 3-fold *fcc* site on the Cu(111) surface: the separation of the I-induced bands from the Cu-3d bands is larger than that of Br-induced bands, which are largely mixed with the Cu-3d bands. Furthermore, the I-induced bands have parabolic-like shapes around the Γ-point , whereas the Br-induced bands are nearly flat along the same path. These findings explain why the Br-induced band cannot be observed distinctively in the ARPES experiment. In addition, the spin-orbit splitting of 0.36 eV between two I-induced bands observed in our calculation is in good agreement with ARPES data. For the Br-induced bands, this splitting is smaller (0.09 eV), indicating as expected that spin-orbit effects for Br are rather small compared to the I atom.

Secondly, when the adsorbates are put on the surface, one of the Cu surface bands goes up in energy, above the Fermi level, meaning that a charge transfer took place from the surface to the halogen atoms. (see SI for the detailed discussion on this point.)

Also, it is noteworthy to mention that both the Cu-3d bands and the I-induced bands measured by ARPES are deeper in energy than in the DFT band structures. This is due to the well known problem of DFT when used with a semi-local approximation for the exchange-correlation potential: it suffers from a self-interaction error, which make the eigenstates to be shifted in energy. This issue could be solved by using a more elaborate level of theory such as hybrid functionals or the GW approximation. However, these methods are computationally heavy, and their use would not change the qualitative comparison bewteen theory and experiments in the present study.

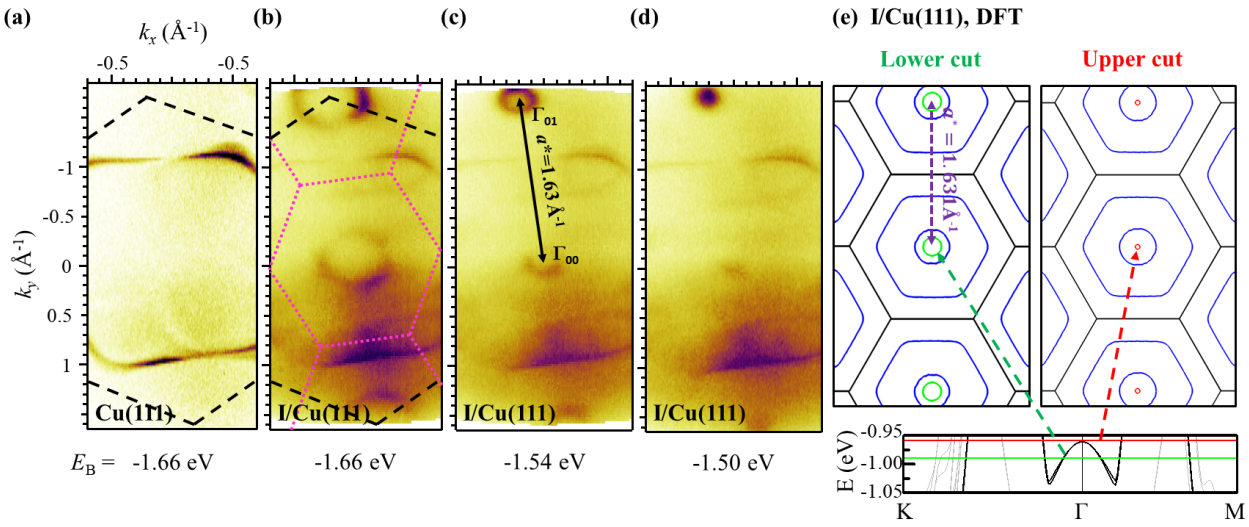

Figure 3: Constant energy maps in the 2-dimensional $\boldsymbol{k}$-space measured by ARPES for (a) the bare Cu(111) surface and (b)-(d) the I/Cu(111) surface taken for three different values of the energy. The black dashed and magenta dotted lines represent the surface Brillouin zone (SBZ) of the clean surface and of the surface with a $(\sqrt{3} \times \sqrt{3})R30^\circ$ overlayer, respectively. Figure 3(e) shows the DFT constant energy maps of the band which contains the I-induced state (depicted as a black solid line in the bandstructure at the bottom of figure). For both upper and lower energy cuts, the smallest circle corresponds to the I-induced state. The black lines represent the SBZ. For details about the two energy values that were chosen, see the main text.

We have also investigated the shape of I-induced band in the surface Brillouin zone (SBZ) by calculating and measuring constant energy maps. Figures 3(a)-(d) are the ARPES constant energy maps for the Cu(111) and I/Cu(111) surfaces, respectively, with the binding energy cut between -1.5 to -1.7 eV. Whereas only a large hexagon-like structure is shown

in the map for the Cu(111) surface as expected for a photon energy of 35 eV (see figure 3(a)), the I/Cu(111) surface has additional circular structures around the Γ-point (see figure 3(b)-(d)), which comes from the parabolic I-induced band as shown in figure 2(a). As expected, the center of this parabolic state is repeated with a 1.63 $Å^{-1}$ periodicity evidencing that these states are the clear signature of the I-induced states associated with the $\left(\sqrt{3}\times\sqrt{3}\right)R30\,^{\circ}$-I surface superstructure. Furthermore, as the magnitude of the binding energy increases, the size of the circle structure increases, indicating that the I-induced bands have a 2-dimensional quadratic nature.

The corresponding constant energy maps obtained from DFT are shown in figure 3(e). To calculate the constant energy maps, and we chose two energy values in our bandstructure, as depicted in the bottom of figure 3(e): one is −0.96 eV (upper cut), which is just below the maximum in energy of the I-induced bands at the Γ-point, and the other is −0.99 eV (lower cut). The smallest circle around the Γ-point corresponds to the circle-like structure of the I-induced band in the ARPES results, of which the size increases as the magnitude of the binding energy increases. A larger circle and hexagon-shape structures, which are depicted as blue lines, are also shown in each DFT constant energy map. These structures correspond to Cu surface bands in our DFT simulations and are not clearly identified by ARPES due to the attenuation of this signal by the presence of the iodine layer at surface.

By going to higher binding energy, we also observed the evolution of the second I-induced band. Figure S2 (b)-(d) are the ARPES constant energy maps taken at the binding energies in a range between -2 to -1.8 eV, showing that the increase of the radius of the circular structure is repeated again from the Γ-point. The ARPES intensity curves taken at the vicinity of $k_x = -0.1$ $Å^{-1}$ and $k_y = 0.0$ $Å^{-1}$ (see figure S2(a)) proves that the second evolution of the circular structure corresponds to the second I-induced band (peak 3).

The origin of the different shapes of the I- and Br-induced bands can be associated with the different size of the Br and I atoms. Since both I and Br have the same $\left(\sqrt{3}\times\sqrt{3}\right)R30\,^{\circ}$ structure on the Cu (111) surface, the nearest Br-Br and I-I distances are the same. However,

the atomic radius of I is larger than the one of Br, resulting in a larger overlap between the nearest I atoms than the nearest Br atoms. This idea is supported by the charge density plots of the I/Cu(111) and Br/Cu(111) overlayers shown in figure S3: our calculated charge densities show that the electrons of I are distributed in a wider region than the electrons of Br. Consequently, the I adsorbates form a band which is more dispersive than the one coming from Br atoms.

Conclusion

In summary, we have studied the geometry and the electronic structure of I/Br atoms adsorbed on a Cu(111) surface by STM, LEED, ARPES measurements combined with DFT simulations. Even if the two halogen elements, I and Br, adsorb at the 3-fold *fcc* site on the Cu(111) surface with a $\left(\sqrt{3} \times \sqrt{3}\right)R30^\circ$ super-periodicity, we found that they display different electronic structure. When Br atoms are adsorbed, the corresponding band presents a flat dispersion and is close to the Cu-3d bands, and, in this particular experimental case, superimposed with molecular states so that ARPES can hardly resolve it. However, the induced spin-orbit splitted bands by the I adsorbate are well separated from the Cu-3d bands. From the analysis of the band structures and of the constant energy maps, we found that the I-induced bands have a quadratic nature in $\boldsymbol{k}$-space, a feature which is shown in both our calculations and our experiments. Overall, the work presented here solves the long standing issue of the electronic structure of heavy halogen atoms on noble metal surfaces. In this respect, it represents a fundamental step towards a better understanding of the complex interplay between reactants and products of the surface mediated Ullmann reaction.

Acknowledgement

The authors acknowledge financial support from the Agence Nationale de la Recherche (ANR) under Grant No. ANR-15-CE29-0003-01, the Italy-France International Program of

Scientific Cooperation (PICS No. 6823, CNRS/CNR), and the French PIA project "Lorraine Université d'Excellence" (LUE). Calculations were conducted using GENCI-CCRT/CINES computational resources (Grant No. x2019-085106).

Supporting Information Available

- supp_info.pdf: supplementary figures and detailed analysis of surface bands

This material is available free of charge via the Internet at `http://pubs.acs.org/`.

References

(1) Magnussen, O. M. Ordered Anion Adlayers on Metal Electrode Surfaces. *Chem. Rev.* **2002**, *102*, 679–726.

(2) Andryushechkin, B. V.; Pavlova, T. V.; Eltsov, K. N. Adsorption of halogens on metal surfaces. *Surf. Sci. Rep.* **2018**, *73*, 83–115.

(3) Pettersson, L. G. M.; Bagus, P. S. Adsorbate ionicity and surface-dipole-moment changes: Cluster-model studies of Cl/Cu(100) and F/Cu(100). *Phys. Rev. Lett.* **1986**, *56*, 500–503.

(4) Koper, M. T.; van Santen, R. A. Interaction of halogens with Hg, Ag and Pt surfaces: a density functional study. *Surf. Sci.* **1999**, *422*, 118–131.

(5) Migani, A.; Sousa, C.; Illas, F. Chemisorption of atomic chlorine on metal surfaces and the interpretation of the induced work function changes. *Surf. Sci.* **2005**, *574*, 297–305.

(6) Migani, A.; Illas, F. A Systematic Study of the Structure and Bonding of Halogens on Low-Index Transition Metal Surfaces. *J. Phys. Chem. B* **2006**, *110*, 11894–11906.

(7) Bagus, P. S.; Käfer, D.; Witte, G.; Wöll, C. Work Function Changes Induced by Charged Adsorbates: Origin of the Polarity Asymmetry. *Phys. Rev. Lett.* **2008**, *100*, 126101.

(8) Bagus, P. S.; Wőll, C.; Wieckowski, A. Dependence of surface properties on adsorbate-substrate distance: Work function changes and binding energy shifts for I/Pt(111). *Surf. Sci.* **2009**, *603*, 273–283.

(9) Peljhan, S.; Kokalj, A. Adsorption of Chlorine on Cu(111): A Density-Functional Theory Study. *J. Phys. Chem. C* **2009**, *113*, 14363–14376.

(10) Pašti, I. A.; Mentus, S. V. Halogen adsorption on crystallographic (111) planes of Pt, Pd, Cu and Au, and on Pd-monolayer catalyst surfaces: First-principles study. *Electrochim. Acta* **2010**, *55*, 1995–2003.

(11) Roman, T.; Groß, A. Periodic Density-Functional Calculations on Work-Function Change Induced by Adsorption of Halogens on Cu(111). *Phys. Rev. Lett.* **2013**, *110*, 156804.

(12) Gossenberger, F.; Roman, T.; Forster-Tonigold, K.; Groß, A. Change of the work function of platinum electrodes induced by halide adsorption. *Beilstein J. Nanotechnol.* **2014**, *5*, 152–161.

(13) Roman, T.; Gossenberger, F.; Forster-Tonigold, K.; Groß, A. Halide adsorption on close-packed metal electrodes. *Phys. Chem. Chem. Phys.* **2014**, *16*, 13630–13634.

(14) Gossenberger, F.; Roman, T.; Groß, A. Equilibrium coverage of halides on metal electrodes. *Surf. Sci.* **2015**, *631*, 17–22.

(15) Zhu, Q.; Wang, S.-q. Trends and Regularities for Halogen Adsorption on Various Metal Surfaces. *J. Electrochem. Soc.* **2016**, *163*, H796–H808.

(16) Chun, H.; Kang, J.; Han, B. Universal Scaling Relationship To Screen an Efficient Metallic Adsorbent for Adsorptive Removal of Iodine Gas under Humid Conditions: First-Principles Study. *J. Phys. Chem. C* **2018**, *122*, 11799–11806.

(17) Citrin, P. H.; Eisenberger, P.; Hewitt, R. C. Adsorption Sites and Bond Lengths of Iodine on Cu{111} and Cu{100} from Surface Extended X-Ray-Absorption Fine Structure. *Phys. Rev. Lett.* **1980**, *45*, 1948–1951.

(18) Jones, R. G.; Kadodwala, M. Bromine adsorption on Cu(111). *Surf. Sci.* **1997**, *370*, L219–L225.

(19) Inukai, J.; Osawa, Y.; Itaya, K. Adlayer Structures of Chlorine, Bromine, and Iodine on Cu(111) Electrode in Solution: In-Situ STM and ex-Situ LEED Studies. *J. Phys. Chem. B* **1998**, *102*, 10034–10040.

(20) Andryushechkin, B. V.; Cherkez, V. V.; Kierren, B.; Fagot-Revurat, Y.; Malterre, D.; Eltsov, K. N. Commensurate-incommensurate phase transition in chlorine monolayer chemisorbed on Ag(111): Direct observation of crowdion condensation into a domain-wall fluid. *Phys. Rev. B* **2011**, *84*, 205422.

(21) Andryushechkin, B. V.; Cherkez, V. V.; Gladchenko, E. V.; Zhidomirov, G. M.; Kierren, B.; Fagot-Revurat, Y.; Malterre, D.; Eltsov, K. N. Atomic structure of Ag(111) saturated with chlorine: Formation of Ag_3Cl_7 clusters. *Phys. Rev. B* **2011**, *84*, 075452.

(22) Zheltov, V. V.; Cherkez, V. V.; Andryushechkin, B. V.; Zhidomirov, G. M.; Kierren, B.; Fagot-Revurat, Y.; Malterre, D.; Eltsov, K. N. Structural paradox in submonolayer chlorine coverage on Au(111). *Phys. Rev. B* **2014**, *89*, 195425.

(23) Cherkez, V. V.; Zheltov, V. V.; Didiot, C.; Kierren, B.; Fagot-Revurat, Y.; Malterre, D.; Andryushechkin, B. V.; Zhidomirov, G. M.; Eltsov, K. N. Self-ordered nanoporous lattice formed by chlorine atoms on Au(111). *Phys. Rev. B* **2016**, *93*, 045432.

(24) Lackinger, M. Surface-assisted Ullmann coupling. *Chem. Commun.* **2017**, *53*, 7872–7885.

(25) Di Giovannantonio, M.; Contini, G. Reversibility and intermediate steps as key tools for the growth of extended ordered polymers via on-surface synthesis. *J. Phys.: Condens. Matter* **2018**, *30*, 093001.

(26) Clair, S.; de Oteyza, D. G. Controlling a Chemical Coupling Reaction on a Surface: Tools and Strategies for On-Surface Synthesis. *Chem. Rev.* **2019**, *119*, 4717–4776.

(27) Björk, J.; Hanke, F.; Stafström, S. Mechanisms of Halogen-Based Covalent Self-Assembly on Metal Surfaces. *J. Am. Chem. Soc.* **2013**, *135*, 5768–5775.

(28) Di Giovannantonio, M.; El Garah, M.; Lipton-Duffin, J.; Meunier, V.; Cardenas, L.; Fagot Revurat, Y.; Cossaro, A.; Verdini, A.; Perepichka, D. F.; Rosei, F. et al. Insight into Organometallic Intermediate and Its Evolution to Covalent Bonding in Surface-Confined Ullmann Polymerization. *ACS Nano* **2013**, *7*, 8190–8198.

(29) Di Giovannantonio, M.; El Garah, M.; Lipton-Duffin, J.; Meunier, V.; Cardenas, L.; Fagot-Revurat, Y.; Cossaro, A.; Verdini, A.; Perepichka, D. F.; Rosei, F. et al. Reply to "Comment on 'Insight into Organometallic Intermediate and Its Evolution to Covalent Bonding in Surface-Confined Ullmann Polymerization'". *ACS Nano* **2014**, *8*, 1969–1971.

(30) Basagni, A.; Sedona, F.; Pignedoli, C. A.; Cattelan, M.; Nicolas, L.; Casarin, M.; Sambi, M. Molecules–Oligomers–Nanowires–Graphene Nanoribbons: A Bottom-Up Stepwise On-Surface Covalent Synthesis Preserving Long-Range Order. *J. Am. Chem. Soc.* **2015**, *137*, 1802–1808.

(31) Björk, J. Reaction mechanisms for on-surface synthesis of covalent nanostructures. *J. Phys.: Condens. Matter* **2016**, *28*, 083002.

(32) Zhou, X.; Bebensee, F.; Shen, Q.; Bebensee, R.; Cheng, F.; He, Y.; Su, H.; Chen, W.; Xu, G. Q.; Besenbacher, F. et al. On-surface synthesis approach to preparing one-dimensional organometallic and poly-*p*-phenylene chains. *Mater. Chem. Front.* **2017**, *1*, 119–127.

(33) Galeotti, G.; Di Giovannantonio, M.; Lipton-Duffin, J.; Ebrahimi, M.; Tebi, S.; Verdini, A.; Floreano, L.; Fagot-Revurat, Y.; Perepichka, D. F.; Rosei, F. et al. The role of halogens in on-surface Ullmann polymerization. *Faraday Discuss.* **2017**, *204*, 453–469.

(34) Vasseur, G.; Fagot-Revurat, Y.; Sicot, M.; Kierren, B.; Moreau, L.; Malterre, D.; Cardenas, L.; Galeotti, G.; Lipton-Duffin, J.; Rosei, F. et al. Quasi one-dimensional band dispersion and surface metallization in long-range ordered polymeric wires. *Nat. Commun.* **2016**, *7*, 10235.

(35) Kresse, G.; Furthmüller, J. Efficient iterative schemes for *ab initio* total-energy calculations using a plane-wave basis set. *Phys. Rev. B* **1996**, *54*, 11169–11186.

(36) Kresse, G.; Joubert, D. From ultrasoft pseudopotentials to the projector augmented-wave method. *Phys. Rev. B* **1999**, *59*, 1758–1775.

(37) Perdew, J. P.; Burke, K.; Ernzerhof, M. Generalized Gradient Approximation Made Simple. *Phys. Rev. Lett.* **1996**, *77*, 3865–3868.

(38) Villars, P.; Daams, J. L. C. Atomic-environment classification of the chemical elements. *J. Alloy. Compd.* **1993**, *197*, 177–196.

Graphical TOC Entry

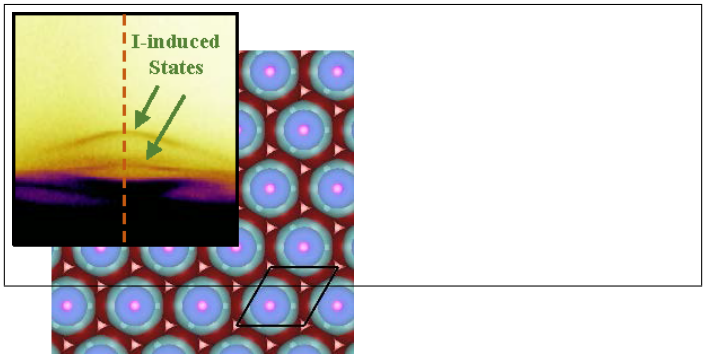

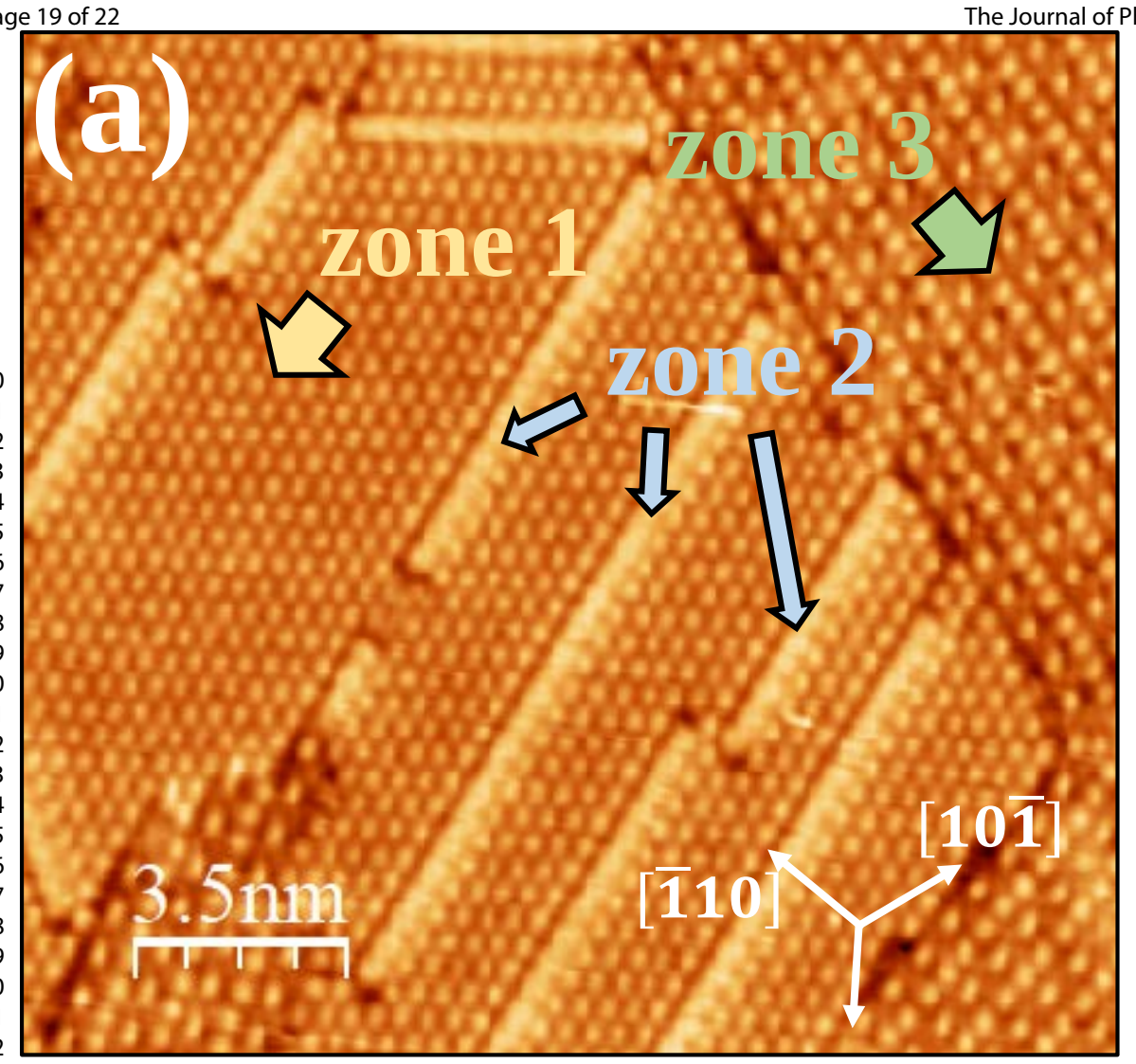
(a)
zone 3
zone 1
zone 2
3.5nm
[$\bar{1}$10]
[10$\bar{1}$]

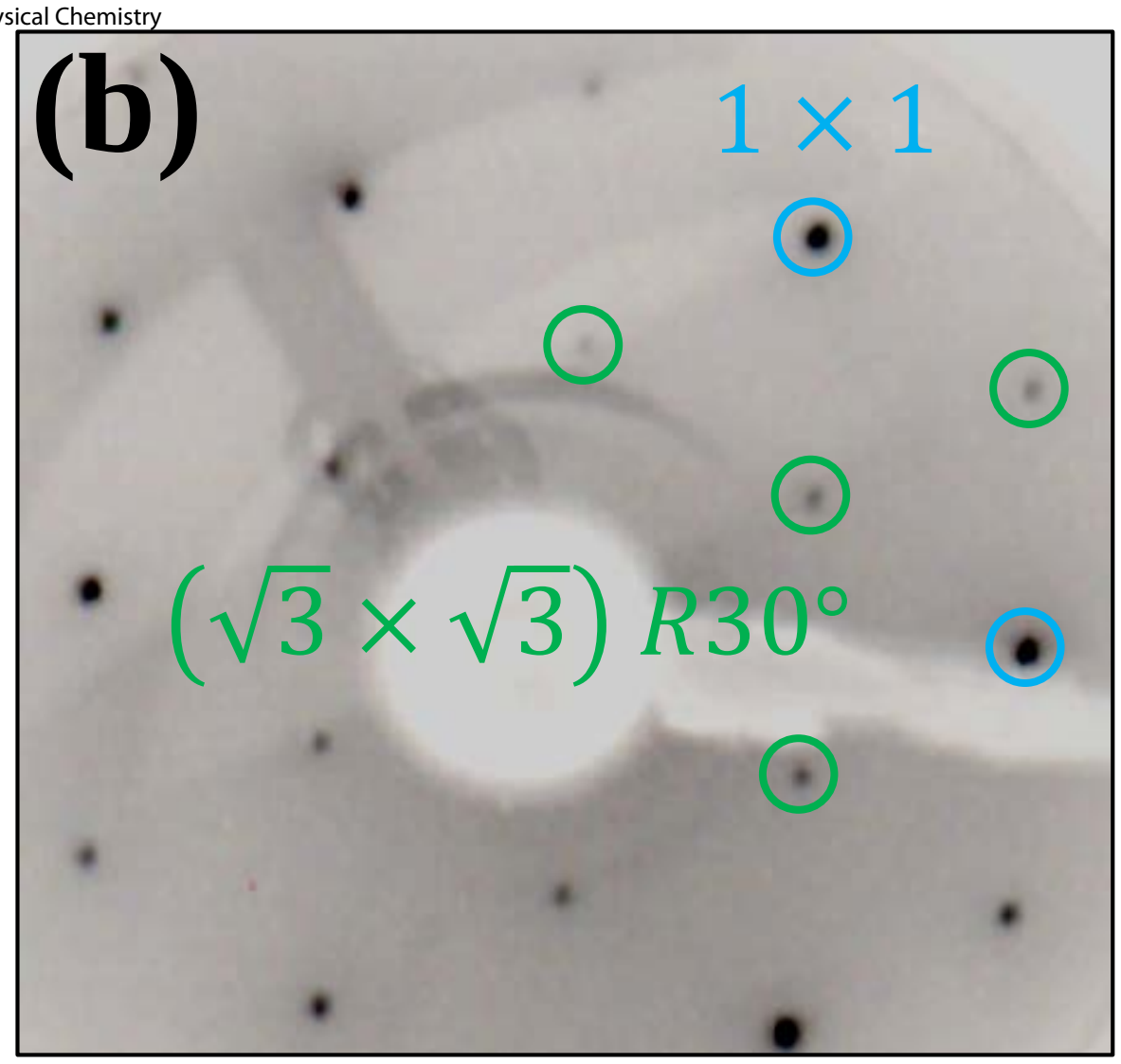
(b)
1 × 1
$(\sqrt{3} \times \sqrt{3})\ R30°$

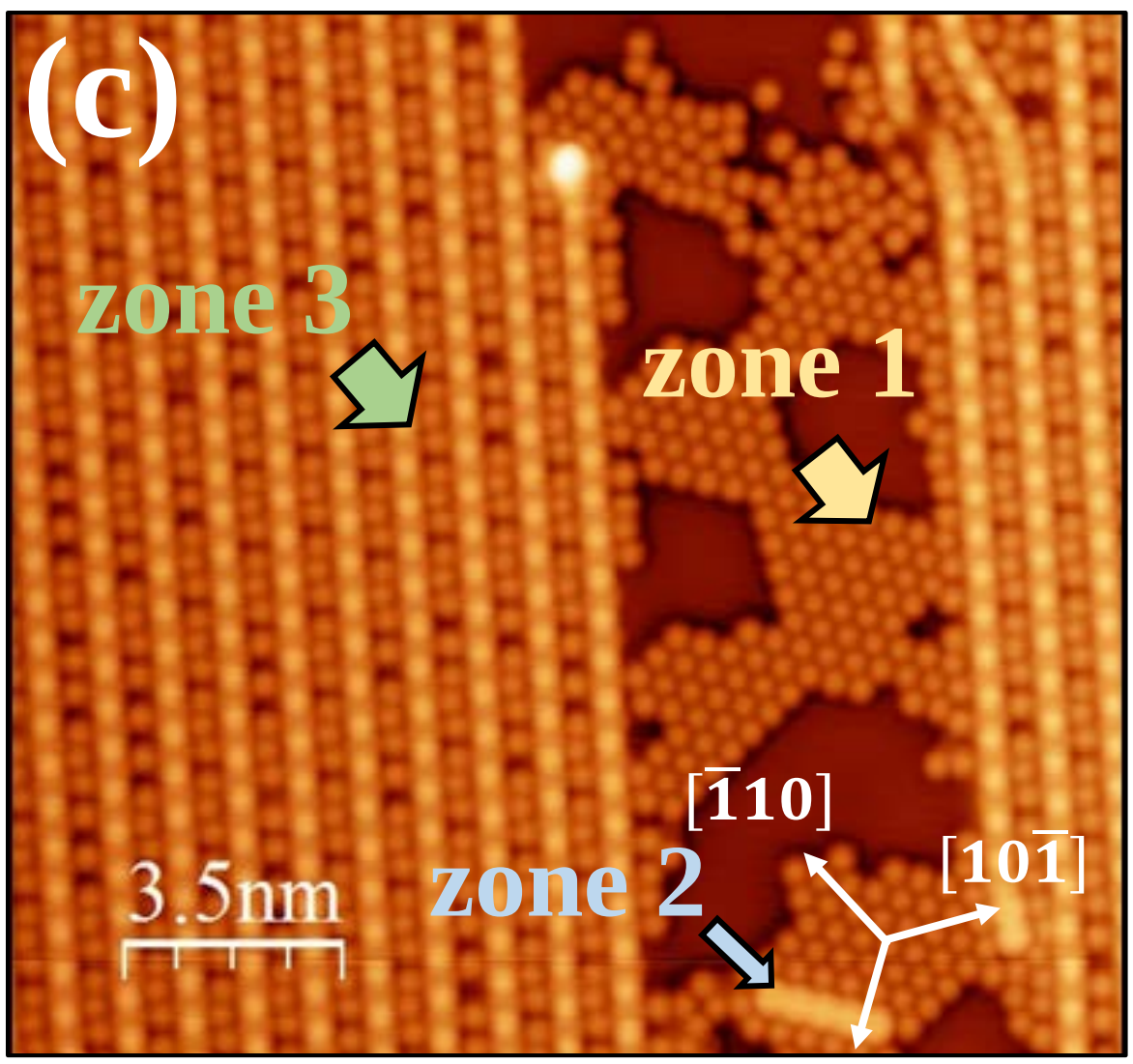
(c)
zone 3
zone 1
zone 2
3.5nm
[$\bar{1}$10]
[10$\bar{1}$]

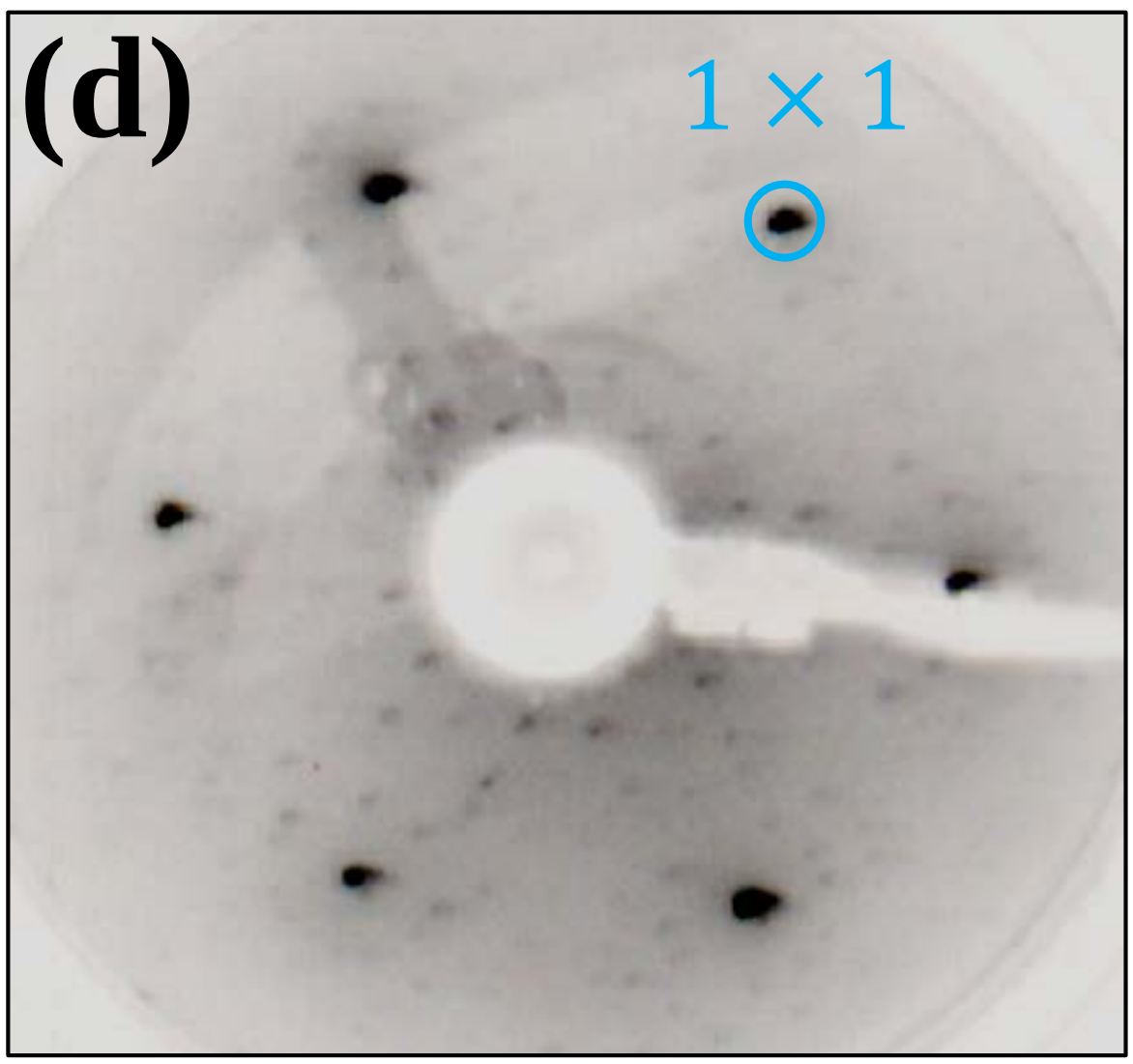
(d)
1 × 1

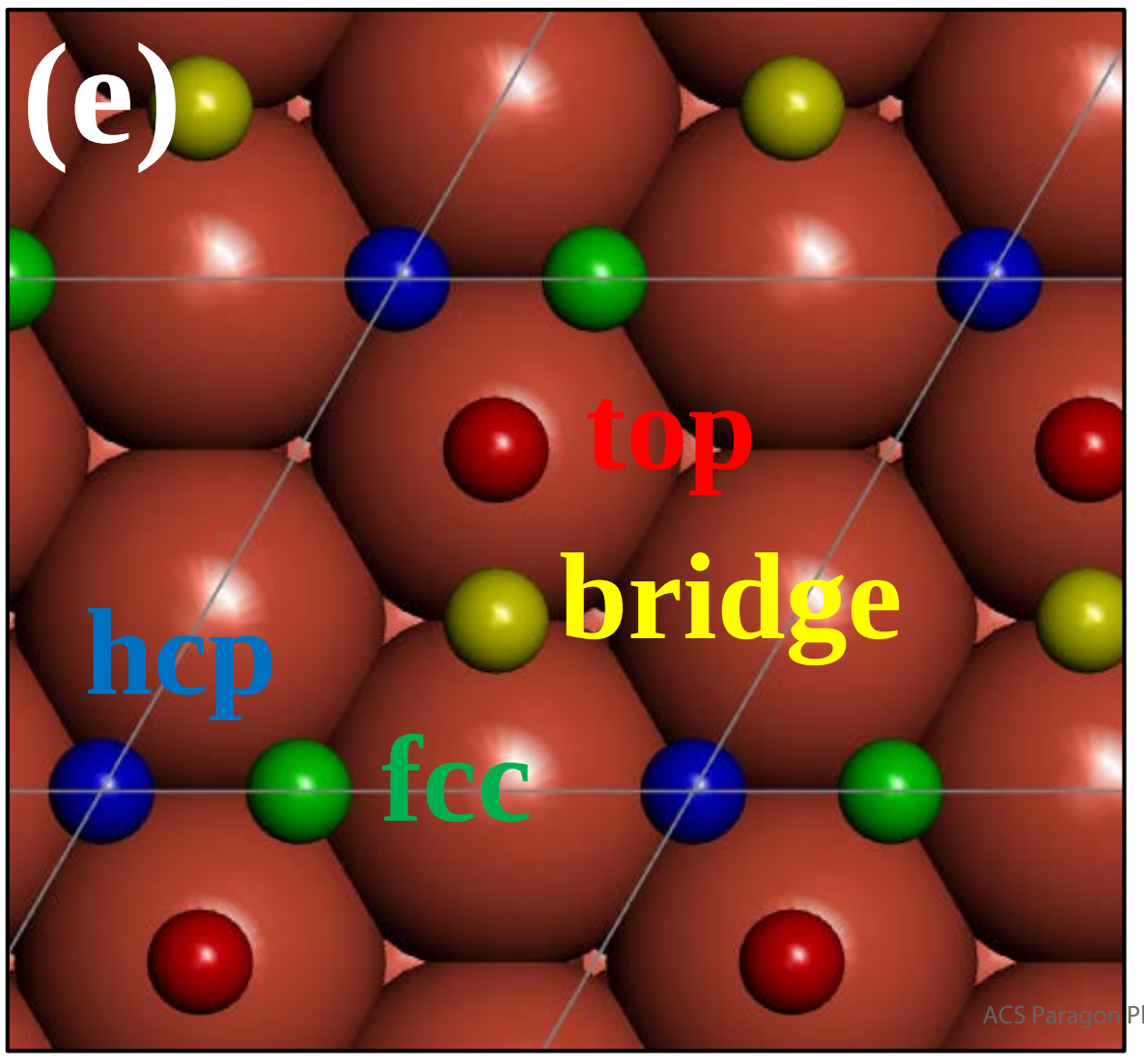
(e)
top
bridge
hcp
fcc

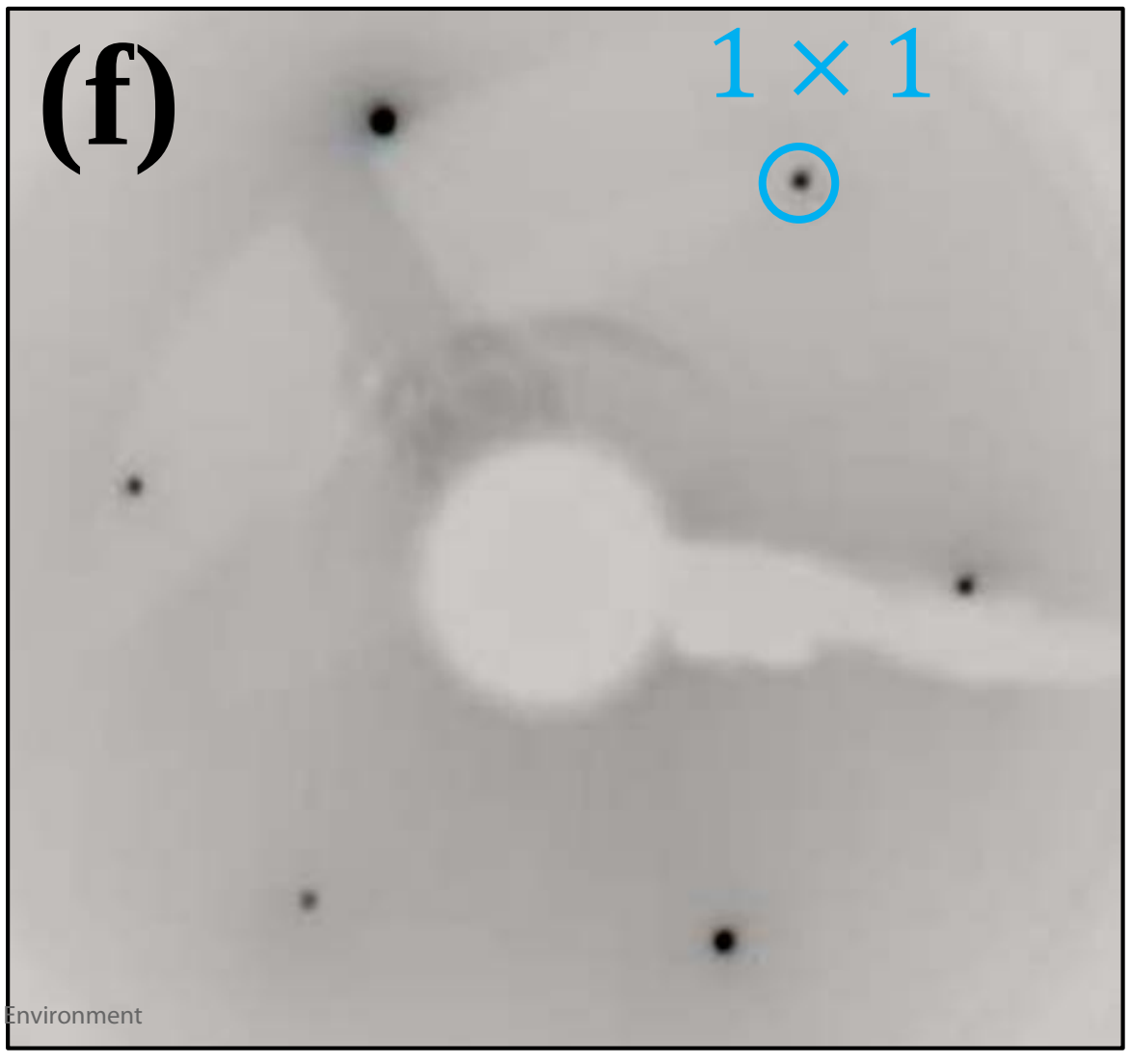
(f)
1 × 1

(a)
I/Cu(111)
ARPES
(d)
I/Cu(111)
DFT
0
-1
-2
-3
Energy (eV)
K'√3
Γ
M'√3
Γ'√3
a*=1.63 Å-1
-0.5
0.0
0.5
1.0
1.5
K
Γ
M
(b)
Br/Cu(111)
(e)
Br/Cu(111)
(c)
Clean Cu(111)
(f)
Clean Cu(111)
M1×1
K1×1
k (Å-1)

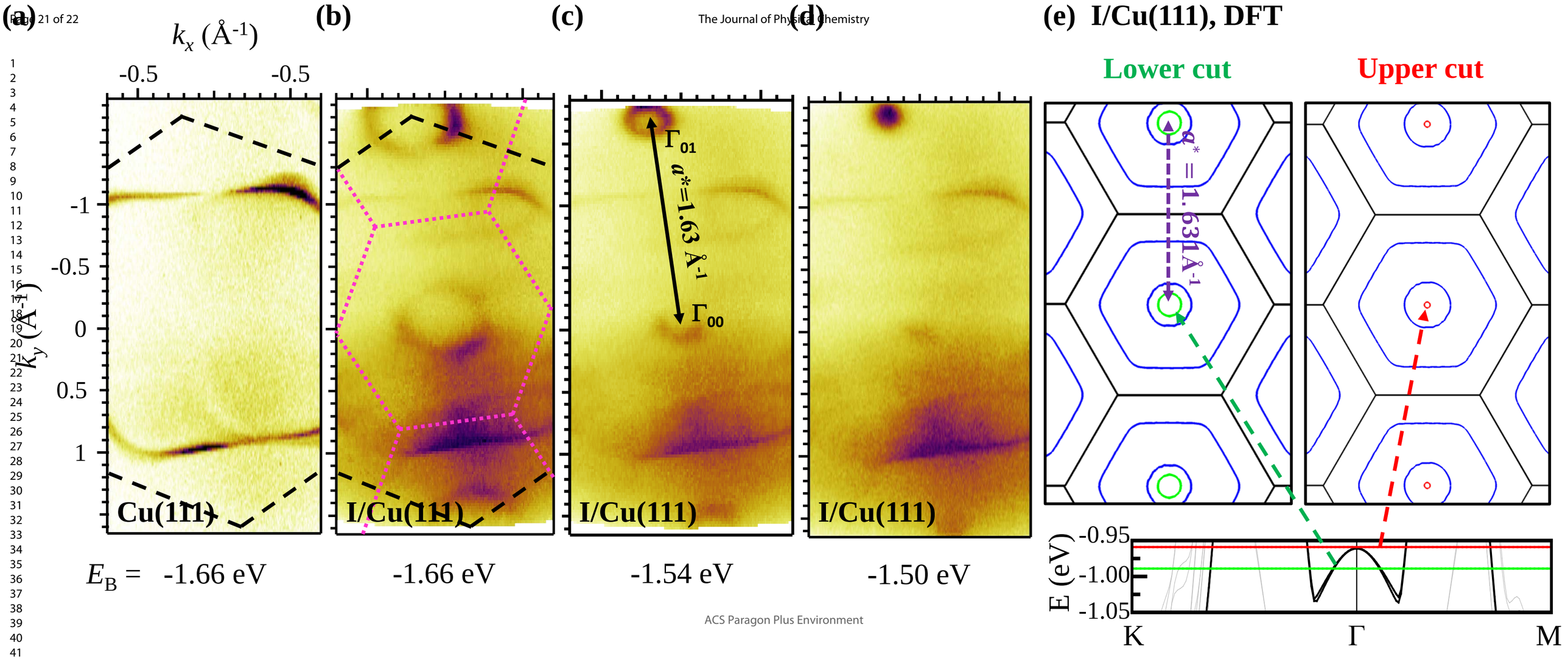
(a)
(b)
(c)
(d)
(e) I/Cu(111), DFT
k_x (Å^{-1})
-0.5
-0.5
k_y (Å^{-1})
-1
-0.5
0
0.5
1
Cu(111)
I/Cu(111)
I/Cu(111)
I/Cu(111)
Γ_{01}
a^*=1.63 Å^{-1}
Γ_{00}
E_B = -1.66 eV
-1.66 eV
-1.54 eV
-1.50 eV
Lower cut
Upper cut
q^* = 1.631 Å^{-1}
E (eV)
-0.95
-1.00
-1.05
K
Γ
M